Determination of Caving Hydraulic Radius of Rock Mass in Block Caving Method using Numerical Modeling and Multivariate Regression

Behnam Alipenhani [1], Abbas Majdi [2*], Hassan Bakhshandeh Amnieh [3]

School of Mining Engineering, College of Engineering, University of Tehran, Tehran, Iran

Article Info	Abstract
	Determining the hydraulic radius of the undercut in the block caving method is one of the key issues in this method. The hydraulic radius is directly related to the minimum caving span. In this research work, the rock mass cavability is investigated using the UDEC and 3DEC software. Since the factors affecting the cavability are very diverse and numerous, firstly, by 2D modeling in the UDEC software and examining the trend of changes in the minimum caving span, the most important factors including the depth, dip of the joint, number of joints, angle of friction of the joint surface, and joints spacing are selected for the final study. The variation trend of each variable is investigated by keeping the other variables constant (single-factor study) among various factors. In the second step, the minimum caving span for the five main factors and values is determined in the single-factor study using the SPSS software and the multivariate regression method. Then the power function of the minimum caving span is chosen based on the selected variables with a coefficient of determination of 0.76. In continuation, a simple 3D model is built from the undercut. A linear equation is achieved between the results of the 3D and 2D modeling results in similar conditions. In a model with certain conditions, using the equation obtained from the numerical method, the calculated hydraulic radius of caving is 22.5 m, which is close to the result obtained from the Laubscher's empirical method with the same condition (24 m).

1. Introduction

The ability of the reliably predicting the undercut dimensions where the initial caving occurs and propagates is essential to the success of this extraction method. Nowadays, this issue is so important since the present studies have reveal that the use of caving methods is essential in hard rock masses as well.

The cavability of the rock mass is defined (often non-quantitative) based on its ability to cave under certain conditions [1] and includes all the three stages of caving, namely initiation, propagation, and continuous caving. The initiation of caving is the start of the rock mass failure that is directly related to its cavability. As soon as the undercut is blasted, the ore column loses its underlying support. Caving begins when failure or collapse occurring in the above area of the undercut. At the same time that the caved material is drawn through

the draw points, the propagation of caving is continued upward in the ore column. It is often necessary to expand the undercut dimensions at which caving begins to prevent a stable arc that stops the continuous caving in the cave back. Arching is the biggest obstacle to the propagation of caving, and creates a stable arc in the cave back. Until a stable arc gets formed, caving may extend for a limited time indicating the initial caving and limited propagation but continuous caving has not occurred yet. Continuous caving is a mode of incessant caving that is the goal of the block caving design. By creating a large undercut to overcome a stable arc continuous caving is also happened. When continuous caving is achieved, the rate of propagation is controlled by the pattern and the draw rate of the broken material [2].

✉ *Corresponding author: amajdi@ut.ac.ir (A. Majdi).*

In the empirical method based on the rock mass classification systems (such as RMR, MRMR, Q and RQD) as well as the gained experiences in open stopes mines, the rock mass cavability has been investigated. Among the empirical methods, the Laubscher caving chart is closer to the industry standards because in this method, both the natural and induced factors affecting the rock mass cavability are included.

The purpose of this work is to investigate the factors affecting the rock mass cavability and to obtain the statistical equation to determine the hydraulic radius of caving based on the most important effective parameters. For this purpose, after introducing the empirical methods and the background of the numerical research in the field, the 2D numerical modeling has been performed to analyze the sensitivity of the effective parameters. After determining the most important parameters affecting the minimum caving span, considering all the selected values for each parameter, all the possible scenarios were modeled. A total number of 480 different modes were examined, and in each mode, the span was changed to obtain a displacement equal to 1 m at the roof. Then the 3D modeling was performed, and the results obtained were compared with the results of the 2D model. By performing a number of 3D and 2D models, the equation between the hydraulic radius and the minimum caving span was determined. The results gained from the Laubscher method were used in order to validate the proposed equation.

2. History of Studies

In general, the methods used for assessing the rock mass cavability and propagation of caving are divided into three categories, namely the analytical, empirical, and numerical ones. Tables 1, 2, and 3 show the history of the performed studies in this field. Since the Laubscher method is used for validation, this method is described.

In 1981, Laubscher proposed a procedure in order to select the appropriate method for underground mass extraction. This selection procedure was based on his rock mass classification system. The Laubscher's method

used the mass mining methods (large caving) against open stoping, and he mainly emphasized upon discussing cavability. The parameters that influenced the selection of the extraction method between the caving and open stope methods were RQD, joint spacing, and joint conditions (degree of weathering, filling and water conditions) [3]. This method emphasized more upon jointing as a determining factor in cavability. In 1990, Laubscher developed the most commonly used method to estimate cavability based on a combination of data from large mines in South Africa. The Laubscher's caving chart illustrates the three possible modes, as follow:

- No caving (stable);

- Transition status: It is a situation in which caving begins but its propagation is low.

- Caving: It is a condition in which continuous caving occurs.

Using this chart and determining the mining rock mass rating (MRMR) and the hydraulic radius of the deposit footprint, the status of the rock mass can be determined. The MRMR system was first introduced by Laubscher in 1974 [5], and was further developed as the extended RMR system by Bieniawski (1976) [6] for the mining activities. In 2000, he made some changes to the calculation process. RQD was removed in the new procedure. The system included the parameters of intact rock strength, discontinuity frequency, discontinuity conditions and weathering adjustment coefficients, joint orientation, induced stresses due to mining, and blasting effects. Finally, Laubscher presented a diagram for the hydraulic radius-MRMR. Although this method is capable of predicting cavability in weak and large deposits, it also has some disadvantages including:

- The accuracy of this graph depends on the homogeneity of the deposit and the reliability of the input data for the MRMR calculation;

- At high MRMR rates (hard rocks) and small deposits, there is a considerable difference between the observed behavior and the predicted behavior [7].

Table 1. History of analytical and empirical methods used for cavability assessment.

Model type	References	Purpose and application
Analytical	Rice and Panek (1948) [8]	Providing a simple 1D volumetric method to investigate the caving propagation behavior by assuming constant coefficients of volume increase
	Ross *et al*. (2005) [9]	Estimation of caving propagation rates at the Northparkes mine in Australia
	Carlson *et al*. (2008) [10]	Estimation of caving propagation rates at Henderson mine, Colorado, USA
	Beck *et al*. (2011) [11]	Estimation of caving propagation rates at ridgeway deeps mine, Australia
	Someehneshin *et al*. (2015) [12]	Determination of the optimal block size in the block caving method by the analytical method
Empirical	King (1945) [13]	Estimation of rock mass cavability based on the rock type, discontinuities spacing, and its mineralogy
	McMahon (1969) [14]	Presentation of the cavability index (CI) to predict the cavability, fragmentation, and secondary blasting requirements using the data from the Climax and Urad mines and establishing a relationship between CI and RQD
	Morison (1976) [15]	Providing a qualitative procedure for selecting the extraction methods in hard rocks
	Laubscher (1981) [16]	Providing a procedure for selecting the underground mass mining method based on the minimum span
	Laubscher (1990) [16]	Presentation of hydraulic radius diagram in MRMR by combining the caving mine data
	Mathew *et al*. (1980) [17]	Presenting a hydraulic radius graph in terms of stability number by combining the caving mine data
	Potvin *et al*. (1980) [18]	Adding the data to the Mathews graph and modifying the stability graph
	Stewart (1980) [18]	Adding the data to the Mathews graph and modifying the stability graph
	Trueman (2000) [19]	Development of the data related to stability, minor and major failures of the studied areas, and application of the Mathews method in a wide range of rock mass characteristics
	Mawdesley (2003) [20]	The method of predicting the spontaneous propagation of caving through the stope stability graph
	Mime *et al*. (2008) [21]	Combining the Mathews graph with the dilution diagram data related to the design of the hanging wall of open stope

3. 2D numerical modeling

The dimensions of the studied model were 1000 m X 350 m. The model which was divided into two parts, the jointed zone (areas with potential for caving) and non-jointed zone (areas without potential for caving) to save the time required for program execution. Figure 1 shows the model geometry. The jointed zone includes the areas with the potential of caving, and as a result, has a higher mesh density. The non-jointed zone has a lower mesh density. The model boundaries have been extended to avoid their effects on the results (4.5 times the maximum span created). This type of mesh geometry and the used dimensions have already been utilized by Vyazmensky *et al*. [47] in the analysis of subsidence resulting from the block caving.

Due to the fact that in most of the previous numerical and experimental studies, three joint sets were included in the model, in the initial model, three joint sets with dips of 20, 70, and 90 degrees were included.

Based on the international caving studies, the height of the ore block was 210 m, the width of the

undercut was 60 m, and its height was 8 m [1]. the undercut (60 m × 8 m) is developed in stages in 2 m increments (in ore block). The height of the waste and overburden was assumed to be 200 m, of which 40 m is specified in the model, and the rest of it is applied as the gravitational stress on the upper boundary of the model. The properties of the ore and the waste are assumed to be the same. In this modeling, it is assumed that the draw operation is done regularly. The sides of the model are restrained along the vertical direction, and the lower part of the model is restrained along the horizontal direction. The model properties are selected based on the characteristics used in the modeling of Vyazmensky *et al*. [47] as well as international caving studies [1]. In the models, the effects of the geometric and strength properties of the joints along with the gravitational stress horizontal to vertical stress ratio and compressive strength of the intact rock on the minimum span for the caving initiation are investigated. A view of displacements at the first steps of simulation is presented in Fig. 2.

Table 2. History of numerical methods used in cavability assessment.

Model type	References	Purpose and application
Continuous	Barla *et al.* (1980) [22]	2D finite element simulation at the Grace Mine in Pennsylvania, USA
	Rech and Loring (1992) [23]	Reproduction of caving conditions at the Henderson mine in Colorado, USA
	Singh *et al.* (1993) [24]	Study of caving at the Rajpura Dariba mine
	Karzulovic *et al.* (1999) [25]	Studying the propagation of caving at the El Teniente mine
	Lorig (2000) [26]	Caving simulation in axial-symmetric models considering cylindrical undercut and lithostatic stress
	Trueman *et al.* (2002) [27]	Determining the amount of stresses in production and undercut production tunnels in some block and panel caving mines as well as the required support system
	Flores and Karzulovic (2003) [1]	Investigation of the effects of depth, stress, large-scale discontinuities, rock mass strength, and groundwater on the cavability by determining the caving propagation factor (CPF)
	Yasitli and Unver (2005) [28]	Evaluation of the abutment pressure around the face and the type of the material flow into the stope
	Pierce *et al.* (2006) [29]	3D Simulation of caving behavior at the Northparkes mine
	Beck *et al.* (2007) [30]	Evaluation of the caving propagation behavior in nickel and diamond deposits using Abaqus
	Gauri Shankar *et al.* (2010) [31]	Investigation of the effects of mining depth, extraction height, horizontal stresses, immediate roof thickness, immediate roof strength, main roof thickness, and main roof strength on the caving behavior
	Wooa *et al.* (2010) [32]	Evaluation of subsidence at the Palabora mine using FLAC3D
	Sainsbury (2012) [2]	Studying the caving propagation and subsidence
	Potvin *et al.* (2018) [33]	Centrifuge modeling of caving mechanism using 3DEC and FLAC3D
	Öge *et al.* (2018) [34]	Prediction of cavability in the Top Coal method using the empirical and numerical methods
	Xia *et al.* (2019) [35]	Investigation of the mechanism of ground pressure damage caused by poor undercutting using FLAC3D
	Xia *et al.* (2020) [36]	Investigation of the mechanism of ground pressure damage process on the extraction opening during deposit extraction by FLAC3D
Distinct Element	Lorig *et al.* (1995) [37]	Using the PFC2D code to better understand the in-situ fracture and improved shape of the cave back
	Brown (2003) [1]	Demonstrating the capacity of the discrete element method to simulate both the caving initiation mechanisms in jointed rock mass (stress and gravity)
	Gilbride *et al.* (2005) [38]	Evaluation of subsidence at the Questa mine using PFC3D
	Kalenchuk (2008) [39]	Prediction of dilution in sub-level caving mine at Ekati Diamond
	Zhao *et al.* (2009) [40]	Simulation of caving process in the TOP coal method using PFC2D
	Sharrock *et al.* (2011) [41]	Modeling caving mechanisms in the large-scale subsidence analyzes
	Gao *et al.* (2014) [42]	Modeling of progressive caving of layers on top of coal mining panel by the long wall method using UDEC
	Rafiee *et al.* (2018) [43]	Investigating the effect of 7 different parameters on cavability using the SRM technique
	Song *et al.* (2019) [44]	Numerical modeling based on 3D particles for process simulation (LTCC)
	Wang *et al.* (2020) [45]	Investigating the effect of top coal block size on the caving mechanism
Hybrid	Yasitli and Unver (2003) [28]	Simulation of the caving process in the block caving method
	Elmo *et al.* (2007) [46]	Discrete fracture network approach applied to the characterization of surface subsidence
	Vyazmensky *et al.* (2010) [47]	Investigation of the role of rock mass fabric and faulting in induced surface subsidence in block caving mines
	Rance *et al.* (2007) [48]	Determination of the amount of *in situ* fragmentation
	Mohammadi *et al.* (2020) [49]	Evaluating the cavability of the immediate roof and estimating the caving span in the long wall method
Other	Tollenaar (2008) [21]	Application of DFN in determining the cavability and fragmentation of rock mass in the block caving mines
	Ivars *et al.* (2011) [50]	Studying the behavior of jointed rock mass using the synthetic rock mass
	Kareka *et al.* (2011) [51]	Application of the SPH methods to simulate the caving process
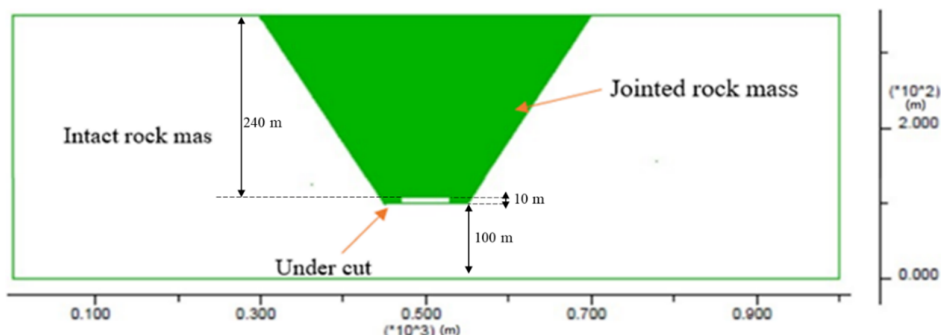
Figure 1. 2D model geometry.

Table 3. History of other methods used in cavability assessment

Model type	References	Purpose and application
Physical modeling	Park and Kicker (1985) [52]	Study of the stress distribution around chain pillar in the long wall method
	Whittaker *et al*. (1985) [53]	Study of mining-induced subsidence by the long wall method, and investigation of the fractures at the upper floors of the stope
	McNEARNY and ABEL (1993) [54]	Study of draw behavior of jointed rock mass in the block caving method
	Carmichael and Hebblewhite (2012) [55]	Analysis of crack propagation and the areas formed in the large caving extraction method
	Potvin (2016) [56]	Analysis of the caving mechanism under the plane strain conditions in a centrifuge experiment
	Jacobsz and Kearsley (2018) [57]	In a centrifuge experiment, the results of placing a weak mass of artificial rock under high and low horizontal stress conditions were examined.
	Bai *et al*. (2018) [58]	In this study, experiments were performed on two large-scale physical models including sand, gravel, gypsum, and mica to investigate the cavability of top coal with hard rock bands based on two real cases.
	Khosravi *et al*. [59]	Investigation of caving mechanism in the block caving method using numerical and physical modeling
Fuzzy rock engineering system	Rafiee *et al*. (2016) [60]	Investigation of the effective factors on cavability using fuzzy system
Rock engineering system	Azadmehr *et al*. (2019) [61]	Estimation of rock mass cavability in the mass caving method using the RES engineering systems method
	Rafiee *et al*. (2015) [62]	Investigation of the factors affecting cavability using rock engineering system (RES)
Probabilistic	Mohammadi *et al*. (2020) [49]	Presenting a probabilistic model for estimating the minimum caving span in the long wall method
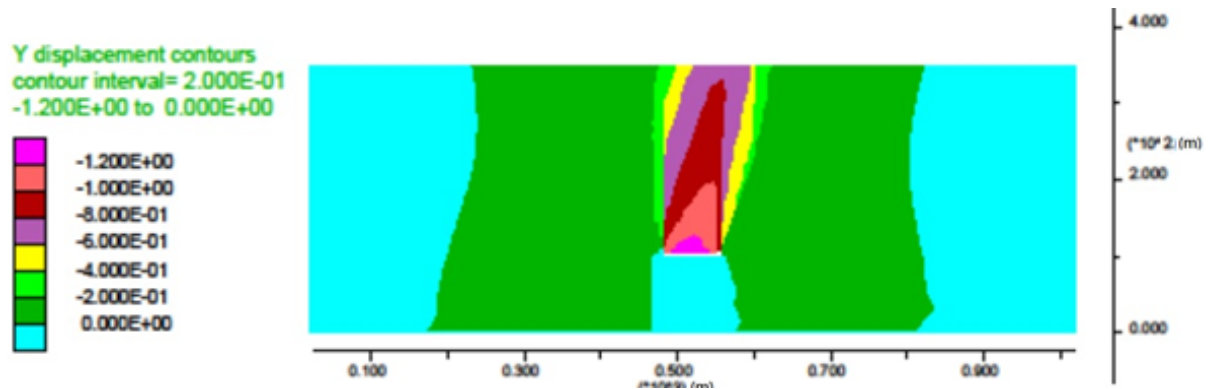
Figure 2. Displacement contours in a model with 60 m length undercut at first steps of solving before undercut.

According to Sainsbury (2012), in the numerical modeling, the caving zone is depicted with a displacement greater than 1 m. This criterion has been selected using the numerical analyses performed at the Northparkes mine in Australia, and has been validated using the results obtained from the Palabora mine in South Africa [2].

The model was solved, and during the solving, the blocks with displacements more than 1 m were removed to simulate the regular and continuous extraction of the caved material. The extracted area and deformation zones in the numerical model are presented in Figure 3.
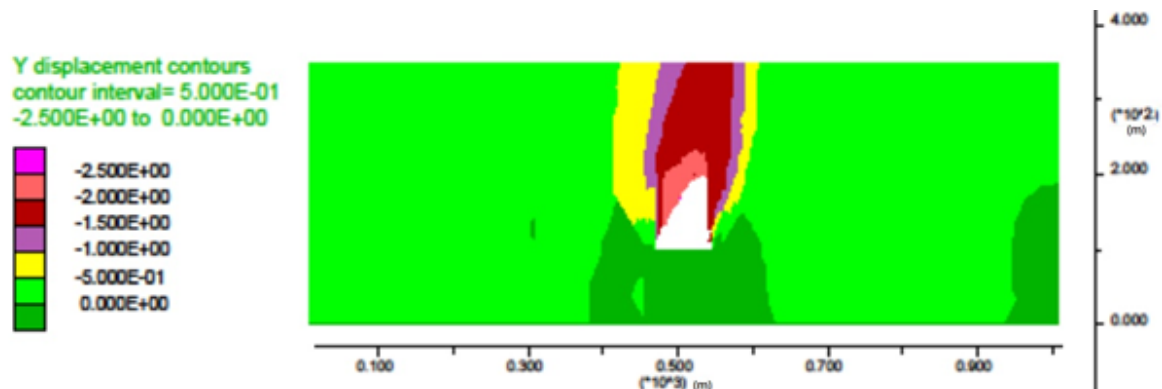
Figure 3. Final cavity and displacement contours around cavity.

3.1. Investigating impact of effective parameters on cavability

A total number of 283 spans were examined in order to find the effects of such parameters as the gravitational stress, horizontal to vertical stress ratio, compressive strength of intact rock, number of joints, cohesion, friction angle, dip, and spacing of joints on the minimum span to initiate caving. In each model, only one parameter was changed and the remaining parameters were considered constant. Table 4 shows the fixed conditions. The criterion for caving initiation is to reach a displacement of 1 m at the roof of the undercut. Per each state, the undercut width was changed until the desired displacement was reached (In 42 models, a total of 283 span with different widths were modeled). Changes in the properties of the joints were applied to all, except the dip. Also the joint properties were changed except for the dip parameter in all the states. In order to perform the sensitivity analysis for the joint dip parameter, only the dip of one joint was changed. The following eight sets of models were built to investigate the effect of the above-mentioned variables on the minimum span of caving:

- Five models to evaluate the effect of mining depth (H)

- Four models to find the effect of horizontal to vertical stress ratio (K)

- Five models to evaluate the effect of compressive strength of intact rock (UCS)

- Four models to evaluate the effect of joint adhesion (Cj)

- Seven models to find the effect of joint friction angle (φj)

- Eight models to evaluate the effect of joint dip (α)

- Seven models to find the effect of joint spacing (S)

- Four models to find the effect of the number of joints (N).

For the final study, a five-factor tree was created. Each tree has values that are based on a single-factor change. Finally, 480 different cases were investigated (Figure 4). In each study, the span was changed till reaching a displacement equal to 1 m at the roof.

Table 4. Fixed conditions in one-factor study of variables.

Intact rock	Value	joints	Value	Parameter	Value
UCS (MPa)	130	Cohesion (MPa)	0	H (m)	500
Density (Kg/m³)	2700	Friction angle (degree)	30	K	1
Cohesion (MPa)	4.7	Normal stiffness (GPa/m)	2	S (m)	3
Friction angle (degree)	45	Shear stiffness (GPa/m)	0.2		
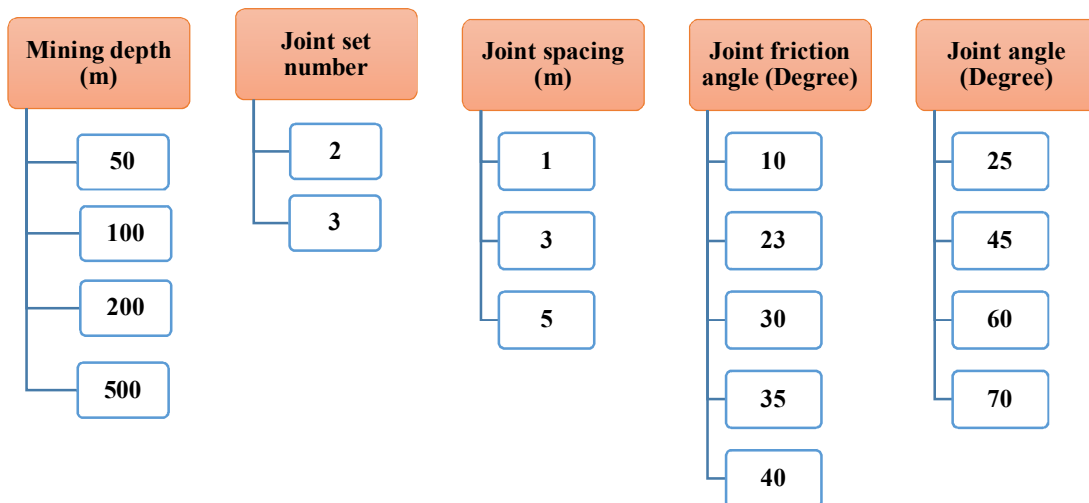
Figure 4. Possible modes for numerical experiments.

The effect of intact rock UCS was investigated using the numerical models. The results obtained indicate that in UCS below 100 MPa, by increasing the unconfined compressive strength, the minimum caving span increases dramatically, while in UCS more than 100 MPa, this parameter is not affected sharply by increasing UCS. According to the results of international caving studies, the average of UCS for underground mines is 130 MPa, and therefore, considering the high values for this factor, this factor has not been considered in the final study. The outcomes of simulations indicate that increasing the 'k' ratio does not affect the displacements of the caving area significantly. On the other hand, the height of the caving area is developed by increasing the undercut span. According to these results, it can be concluded that the 'k' ratio does not affect the cavability of rock mass significantly. Therefore, its value was decided to be constant at one. In most references, the amount of cohesion of joint surface is considered zero. The result shows that the dimension of caving span does not change with the change of cohesion. However, due to the small amount of this variable and the lack of effect in this range (0-0.4 MPa), this factor was not studied in the final study. The results obtained are shown in Figure 5.
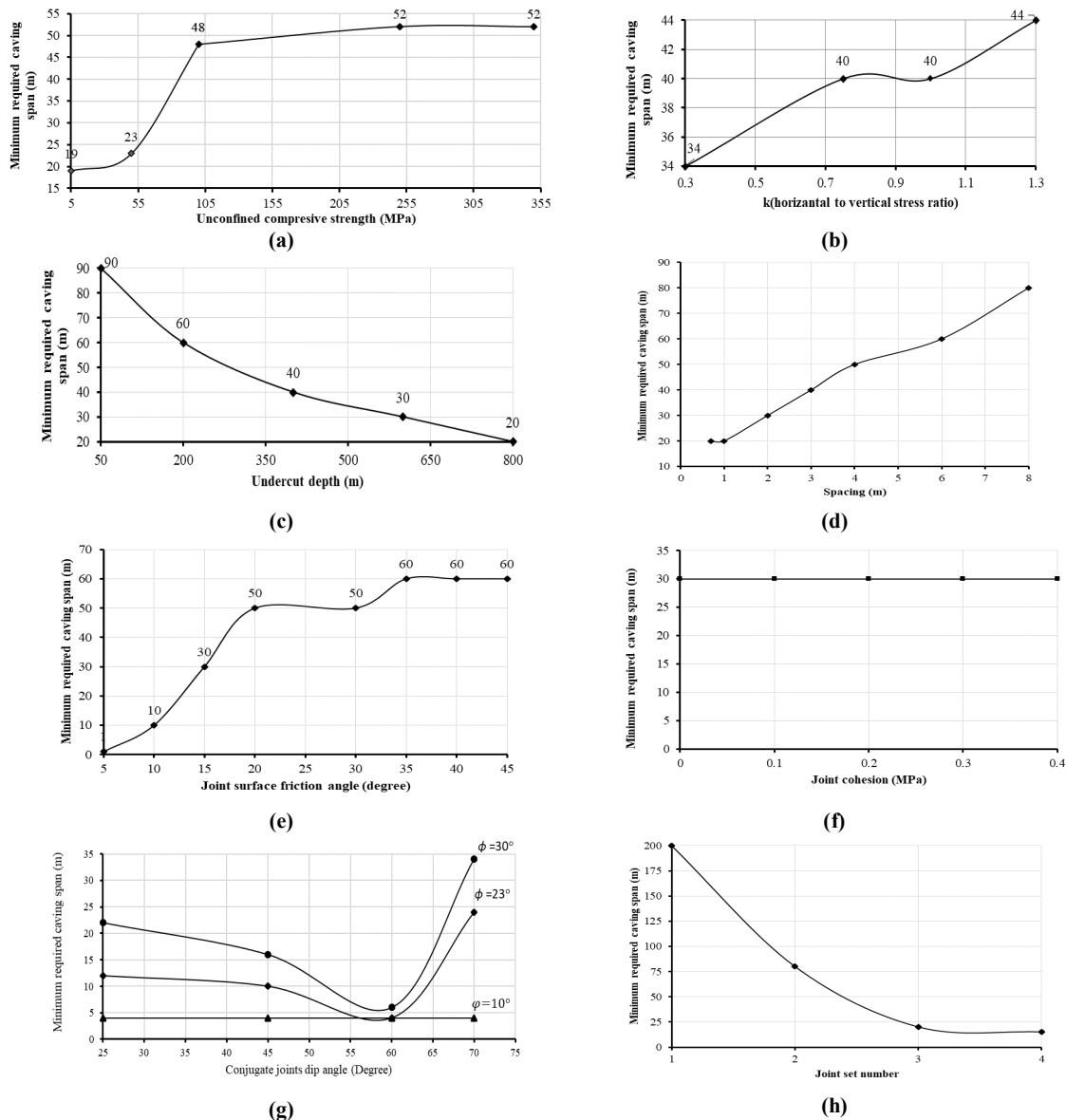
Figure 5. Effect of a) UCS, b) horizontal to vertical ratio, c) depth, d) joint spacing, e) joint friction, f) joint cohesion, g) joint set dip, and h) joint set number on minimum caving span.

3.2. Statistical investigation of 2D modeling results

Table 4 shows an example of the findings at this step. In the numerical modeling, the range of changes of the minimum caving span from 2 to 100 meters was obtained. Multivariate regression is used in order to predict the minimum caving span in terms of the dependent variables. By performing regression in the SPSS statistical software, the

equations listed in Table 5 were obtained for the minimum caving span based on the variables.

In these equations, S_{min} is the minimum caving span in meters, N is the number of joint sets, H is the depth in meters, S is the joint spacing in meters, α is the friction angle of the joint surface in degrees, and D is the dip of the joint in degrees. The analysis showed that the best model was the power regression model obtained according to Equation 6.

Table 4. Representative samples of 480 numerical models input data and the results of numerical simulation.

Model No.	Joint set number (N)	Undercut depth (H, m)	Joint spacing (S, m)	Joint friction angle (α, degree)	Joint inclination (D, degree)	Minimum required caving span (S_{min}, m)
1	3	100	5	10	60	6
2	3	100	5	10	25	8
3	2	200	1	10	25	2
4	3	50	1	23	45	3
5	3	200	5	10	60	5
6	3	50	1	30	45	14
7	2	100	1	40	60	12
8	3	50	5	23	45	26
9	2	50	3	30	45	32
10	2	50	5	10	25	14
11	2	200	3	35	45	27
12	3	50	1	30	70	36
13	3	50	5	23	70	46
14	3	50	5	30	70	62
15	3	50	5	35	60	30
16	3	200	5	35	70	54
17	2	50	3	40	70	76
18	2	200	5	40	70	90
19	2	100	5	35	70	84
20	2	50	5	35	70	98

Table 5. Statistical Equations to determine minimum caving span.

No. of equation	R^2	Equation
(1)	0.63	$S_{min} = 2.47 - 6.13N - 0.038H + 5.58S + 1.016\alpha + 15D$
(2)	0.76	$S_{min} = 10^{0.68 - 0.15N - 0.009H + 0.13S + 0.026\alpha + 0.0021D}$
(3)	0.76	$S_{min} = e^{1.58 - 0.34N - 0.002H + 0.3S + 0.62\alpha + 0.005D}$
(4)	0.59	$S_{min} = 16.83 - 0.03N^5 + 0.031S^4 + 0.0046\alpha^3 + 0.0021D^2 - 0.038H$
(5)	0.6	$S_{min} = 48.37 - 15.12\ln(N) - 17.8\ln(H) + 13.18\ln(S) + 20.94\ln(\alpha) + 4.19\ln(D)$
(6)	0.767	$S_{min} = 43.11N^{-0.842}H^{-0.933}S^{0.740}\alpha^{1.303}D^{0.12}$

The F-test was performed based on the analysis of variance for regression. The corresponding values of Sig and F in Equation 6 are 7.5×10^{-12} and 314.415, respectively. The Sig factor is used to investigate the existence of a linear relationship between the independent variables and the dependent ones. In other words, it shows that at least one of the independent variables has a linear relationship with the dependent variable. In the present equation, the value of Sig is less than 5% (95% confidence level is considered); that is at least one of the independent variables has a significant effect on the dependent variable. In order to have a zero correlation between the model errors, the Durbin-Watson coefficient should be in the range of 1.5-2. This coefficient obtained for the

resulting equation is equal to 2.017, which indicates that the errors are not correlated.

Another assumption considered in the regression is the normality of error distribution with a mean of zero. For this purpose, the standard values of errors must be calculated. Figure 6 shows the frequency distribution of errors and the normal distribution, which has a mean close to zero and a standard deviation of 0.995. As a result, this distribution can be considered as a normal one. The absolute value of the standardized column coefficients shows the effect of each independent parameter on the dependent variable. It is observed that the friction angle of the joint surface has the greatest effect on the minimum caving span. The statistical coefficients for Equation 6 are given in Table 6.

Table 6. Statistical coefficients for Equation 6.

Parameter	Non-standardized coefficients		standardized coefficients	t	Sig
	Std. Error	b			
a	0.536	43.11	-	7.024	
N	0.109	-0.842	-0.171	-7.712	7.35e-14
H	0.076	-0.933	-0.273	-12.327	1.76e-30
S	0.033	0.74	.4980	22.457	1.32e--76
α	0.045	1.303	0.643	29.013	3.75e-137
D	0.056	0.12	0.047	2.132	0.033
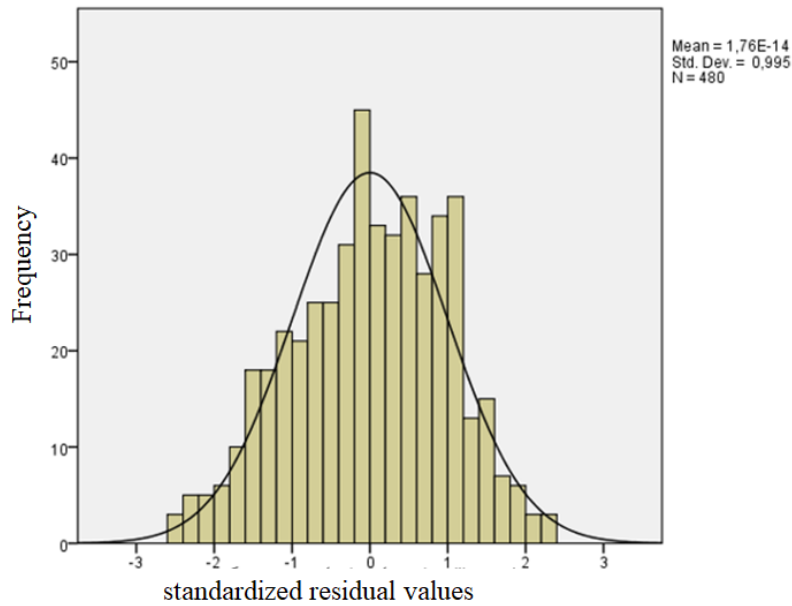
Figure 6. Probability distribution of standardized residual values.

In order to compare the results of Equation 6 and those of the direct modeling, different values that had not been used in the previous modeling were utilized for the variables. Figure 7 shows this comparison. It can be seen that the values obtained from the formula are close to the values obtained from the direct modeling. For the lower values of caving span, the values are closer to each other but for the larger values, they are more scattered.
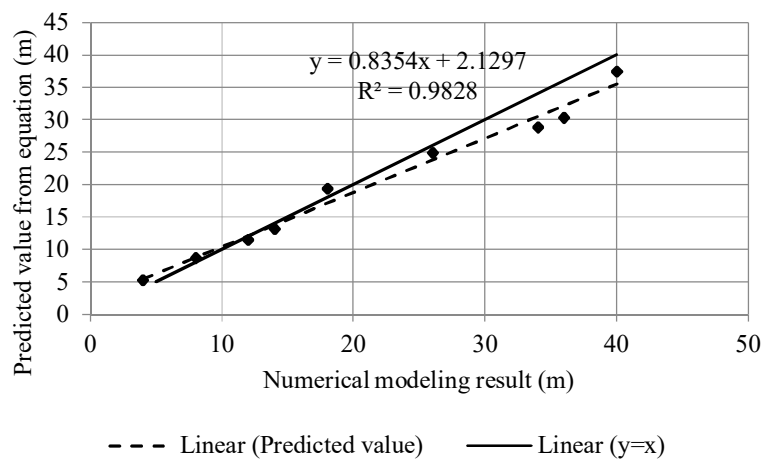
Figure 7. Caving span prediction diagram using Equation 6 according to the result of direct modeling.

4. Caving Hydraulic radius investigation

In 3D modeling, a simple undercut model is considered in the block caving method. In this model, which is built in the 3DEC software, only the beginning of the caving is shown. In other words, the hydraulic radius of the square undercut is changed to the extent that the roof blocks reach a displacement equal to 1 m. In continuation, the longitudinal and transverse sections of the center are given. As it can be seen, the amount and shape of the displacements are the same in both sections, indicating the model symmetry. In addition, it can be concluded that the form of caving is dome-shaped. The corresponding 2D modeling is performed, and the corresponding results are given below.

4.1. 3D numerical modeling

The studied model had the length and width of 1000 m and a height of 350 m. The mode was divided into two parts, with and without joints, to save the computation time, and also due to the limited software memory. Figure 6 shows the model geometry. The joint covers the areas that

have the potential for caving, and as a result, have a higher mesh density.

In the built model, three joint sets were inserted (Figure 8). The dip of the two joint sets is 90 degrees with the dip directions of 0 and 90 degrees, and the joint set is horizontal. The joints inserted in the model are inserted continuity and without aperture, due to the limited memory of the software, with a spacing of 5 m.

According to the caving studies performed worldwide, the c ore block height was considered to be 210 m, and also the length and width of the undercut were 100 m and its height was 8 m [1]. The undercut is created at 20 m × 20 m increments in the model. The height of the waste and overburden were assumed to be equal to 200 m, of which 40 m was specified in the model, and the rest of it was the input as a gravitational stress on the upper bound of the model. The properties of the mineral and the waste were assumed to be the same (Table 7). In this modeling, it is assumed that the drawing is done regularly. In other words, the amount of draw will be the same in all the draw points.

(a)

(b)
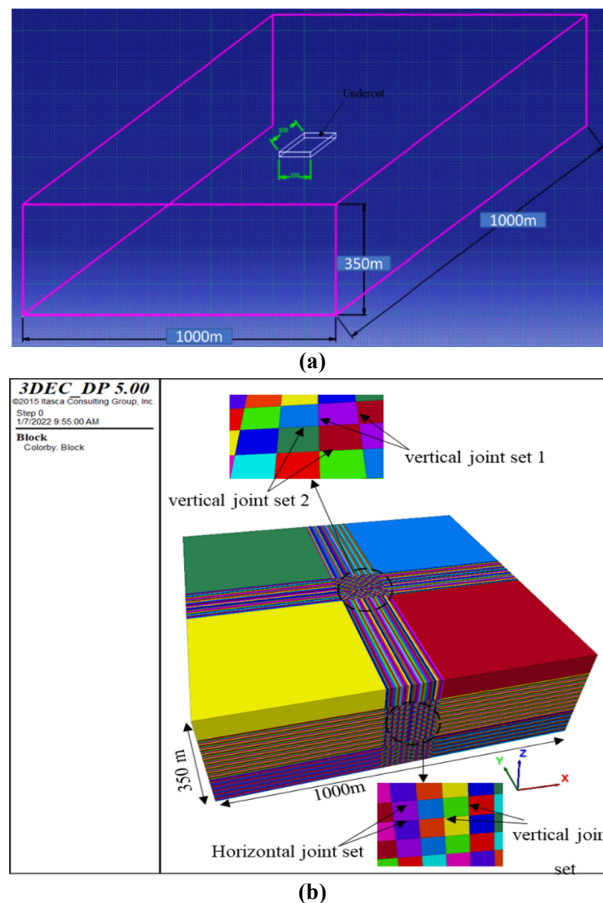
Figure 8. Final geometry of 3D model; (a) Schematic model, and (b) 3DEC model.

Table 7. Input parameters of 3D model [47].

Parameter Intact rock	value	Parameter joints	value	K
UCS (MPa)	100	Cohesion (MPa)	0	1
Density (Kg/m³)	2700	Friction angle (degree)	30	
Cohesion (MPa)	4.7	Normal stiffness (GPa/m)	2	
Friction angle (degree)	45	Shear stiffness (GPa/m)	0.2	

In the prototype model, the initial caving occurred due to the resulting displacements. The model made with a hydraulic radius of 25 m had a displacement greater than 1 m (Figure 9). Since the goal was to reach a displacement of 1 m to start the caving, a new model was built with the 90 m × 90 m undercut dimensions (22.5 m hydraulic radius). Figures 10 and 11 show the vertical displacement along the longitudinal and transverse sections of the new model, respectively, in which a displacement of 1 m has occurred. In other words, the caving initiate at the hydraulic radius of 22.5 m. Next, a 2D model corresponding to the 3D conditions was built. The minimum caving span in the 2D model was 68 m (Figures 12 and 13).
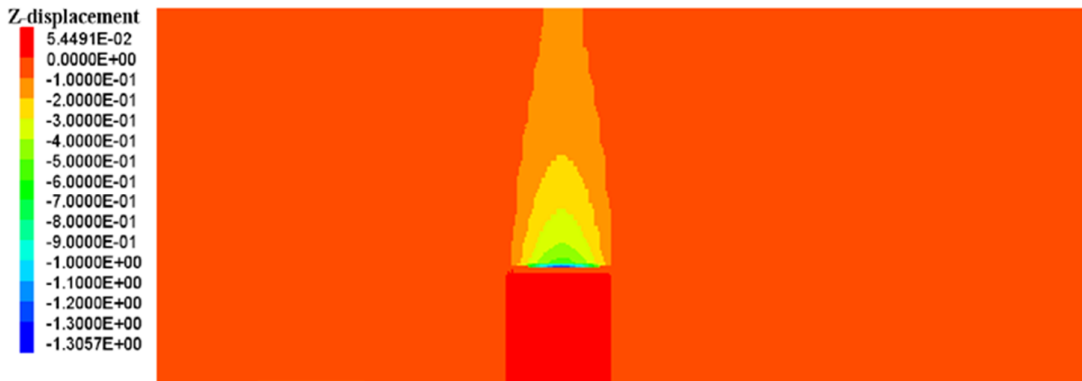
Figure 9. Diagram of displacement of a model with a hydraulic radius of 25 m.
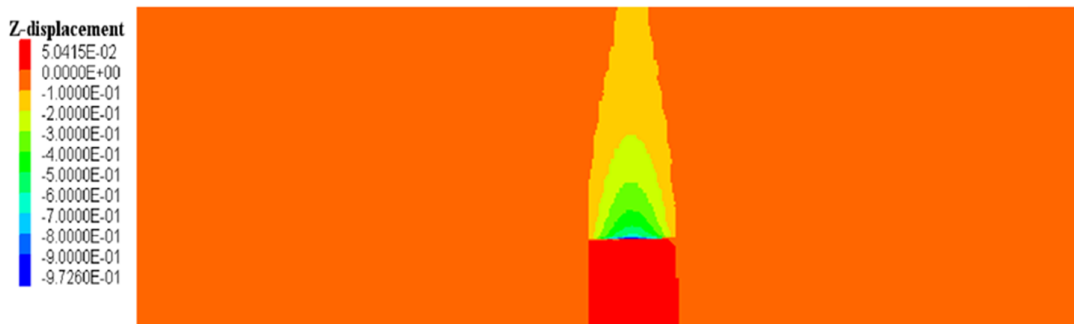
Figure 10. Longitudinal displacements (x direction) of a model with a hydraulic radius of 22.5.
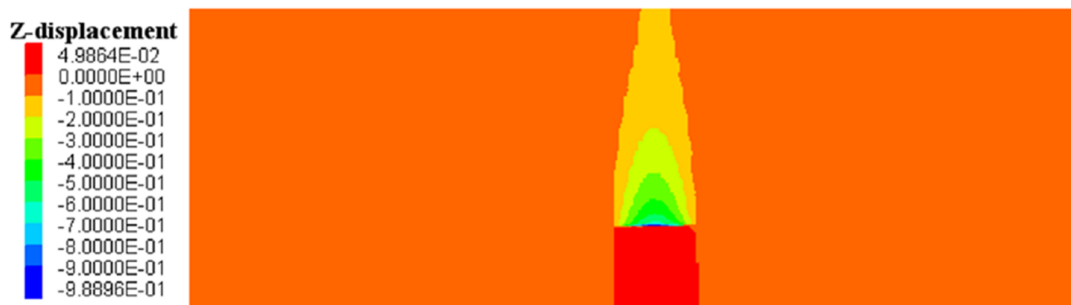
Figure 11. Longitudinal displacements (y direction) of a model with a hydraulic radius of 22.5.
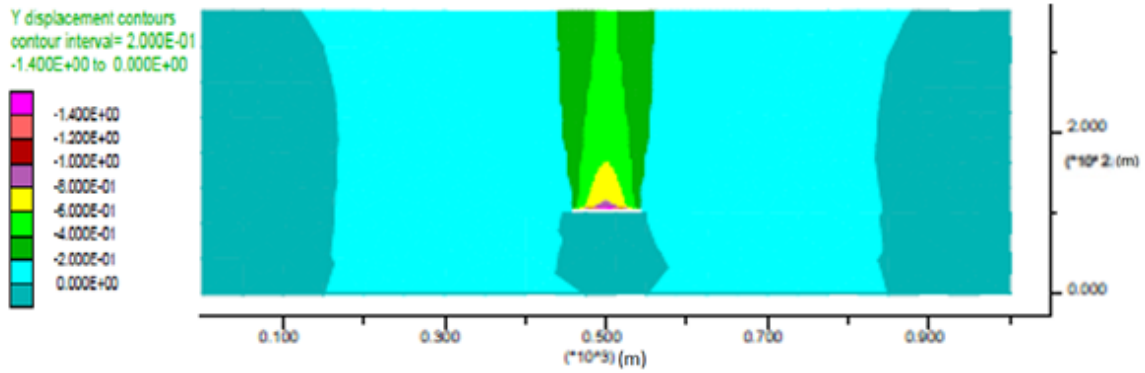
Figure 12. 2D model with a span of 90 m.
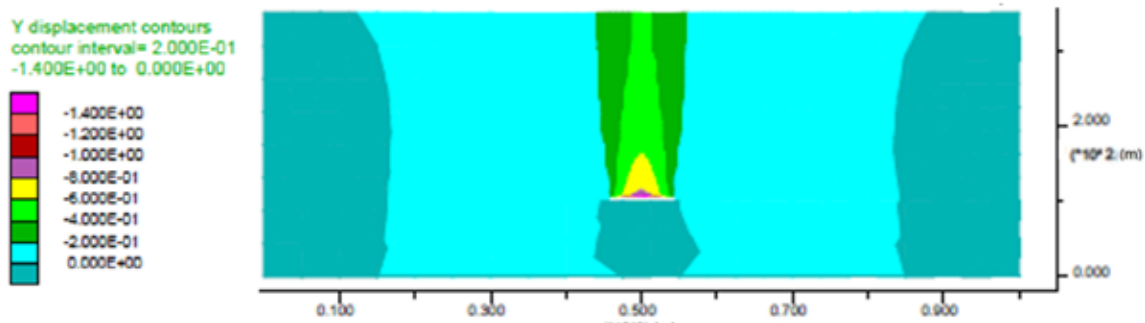
Figure 13. 2D model with a span of 68 m.

4.2. Determination of caving hydraulic radius using Laubscher chart

In this section, incorporating the parameters listed in Table 7, the hydraulic radius of caving was estimated using the Laubscher chart. In Table 8, the MRMR classification of rock mass was calculated step by step with respect to the conditions of Table 7. The total rate was approximately 46, which according to the Laubscher chart showed an approximate hydraulic radius of 24 m. This value is close to the number of hydraulic radii obtained from the numerical modeling (22.5 m) (Figure 14).

Table 8. Determination of MRMR based on 3D numerical model conditions.

Factor	Calculated values	rate
Rock block rate	RBS = 0.8 × IRS = 0.8 × 100 = 80	20
joint spacing	5m	35
Joint condition	C =0 and $\varphi = 30$ (40×0.9×0.75=27)	27
Orientation adjustment	The number of joints that set make up block 3 and the number of plates they make with a right angle is 2, and therefore the correction percentage is 0.8.	0.8
Water adjustment	An environment without water is considered.	1
Blasting adjustment	-	1
Weathering adjustment	An environment without weathering is considered.	1
induced stresses adjustment	Depth of 400 meters and as a result the correction factor is 0.7	0.7
Sum of rates	82	
MRMR	82 × 0.8 × 0.7 = 45.92	46
RBS = Rock block strength, IRs = Intuit rock strength		
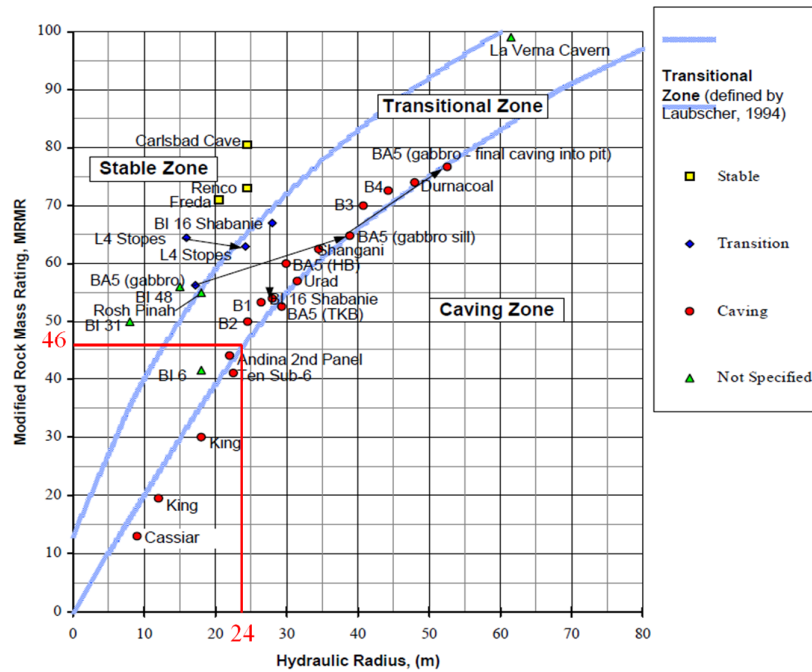
Figure 14. Calculation of hydraulic radius in numerical modeling.

4.3. Determination of caving hydraulic radius based on minimum span

In order to establish a relationship between the minimum caving span and the hydraulic radius of the caving, several 2D and 3D models with the same conditions were built. In these models, all the parameters were applied according to Table 4, and only the friction angle of the joints was changed. The friction angles of 10, 20, 30, and 40 were considered. As shown in Figure 13, the hydraulic radius has a linear relationship with the minimum caving span.
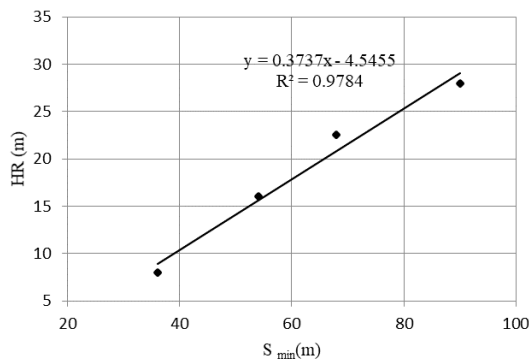
Figure 15. Hydraulic radius-minimum caving span graph.

Taking into account the conditions of Table 7 and the friction angle of 25 degrees, the MRMR value was (similar to Table 8) equal to 36, which resulted

in a hydraulic radius of 18 m. By placing this hydraulic radius in the equation shown in Figure 15, the minimum caving span of 60 m was obtained. By placing the conditions of Table 8 in Equation 6, the minimum caving span was 57.92 m. There is a good agreement between the modeling results and the Laubscher method.

5. Conclusions

- Among the investigated factors, the uniaxial compressive strength of rocks and the horizontal to vertical stress ratio have minimal effects on the minimum caving span.

- Mainly, the effect of five prominent parameters including the joint set number (N), joint spacing (S), joint inclination angle (α), joint surface friction angle (φ), and undercut depth (H) were simulated numerically, and the effects of these parameters on the minimum caving span for the initiation and continuation of the caving process through the ore body were studied.

- Totally, 480 numerical models were simulated with a wide range of input parameters for each model.

- The maximum caving span is related to the condition of two joint sets with a dip of 70 degrees, a friction angle of 40 degrees, a depth of 50 m, and a distance of 5 m.

- The minimum caving span is related to the conditions of two intersecting joint sets with the dips of 60 degrees, friction angles of 10 degrees,

depth of 400 m, and spacing of 1 m. The joint angle of friction has the greatest effect on the minimum caving span.

- As the joint spacing decreases, the depth and number of joint set increase, and the minimum caving span decreases. The rock mass with joints having a dip of 60 degrees has the highest potential for caving. For values less than and greater than 60 degrees, cavability decreases.

- From the functions fitted to the data, a power function with $R^2 = 0.767$ was selected in order to estimate the minimum caving span. Comparison of the results of the 2D modeling and the minimum caving span calculated from the formula showed that the mean value of the errors was approximately equal to 12%.

- A linear equation between the hydraulic radius of caving and minimum caving span was obtained by changing the angle of friction of the joints with a coefficient of determination of 0.97. Assuming a minimum span of 68 m, the hydraulic radius is approximately equal to 21 m (from formula), which is in good agreement with the result obtained from the empirical Laubscher method (24 m).

References

[1]. Brown, E.T. (2003). Block Caving Geo-mechanics. The International Caving Study I. JKMRC Monograph Series in Mining and Mineral Processing 3. University of Queensland.

[2]. Sainsbury, B. (2012). A model for cave propagation and subsidence assessment in jointed rock masses. University of South Wales.

[3]. Darling, P. (Ed.). (2011). SME mining engineering handbook (Vol. 1). SME.

[4]. Laubscher, D. (2000). Cave Mining Handbook.

[5]. Charles A. Brannon, Gordon K. Carlson, and T.P.C. (2011). Block Caving and Cave Mining. SME mining engineering Handbook (Vol. 1). SME.

[6]. Bieniawski, Z.T. (1976). Rock mass classification in rock engineering applications. In Proceedings of a Symposium on Exploration for Rock Engineering, 1976 (Vol. 12, pp. 97-106).

[7]. Brown, E.T. (2002). Block caving geomechanics.

[8]. Rice, G.S. (1934). Ground movement from mining in Brier Hill mine, Norway, Michigan. Mining and Metallurgy, 15(325), 12-14.

[9]. Panek, L.A. (1984). Subsidence in undercut-cave operations, subsidence resulting from limited extraction of two neighboring-cave operations. Geomechanical applications in hard rock mining, 225-240.

[10]. Carlson, G., and Golden, R. (2008). Initiation, Growth, Monitoring and Management of the 7210 Cave at Henderson Mine-A case study. In 5th International Conference and Exhibition on Mass Mining (Vol. 9, pp. 97-106).

[11]. Beck, D., Sharrock, G., and Capes, G. (2011). A coupled DFE-Newtonian cellular automata scheme for simulation of cave initiation. In Propagation and Induced Seismicity. 45th US Rock Mechanics/Geomechanics Symposium Held in San Francisco, CA.

[12]. Someehneshin, J., Oraee-Mirzamani, B. and Oraee, K. (2015). Analytical model determining the optimal block size in the block caving mining method. Indian Geotechnical Journal, 45(2), 156-168.

[13]. Mahtab, M.A., and Dixon, J.D. (1976). Influence of rock fractures and block boundary weakening on cavability. Trans Soc Min Eng AIME. 260 (1): 6-12.

[14]. McMahon, B.K., and Kendrick, R.F. (1977). Predicting the block caving behavior of orebodies. Society of Mining Engineers of AIME.

[15]. Carter P.G. (2011). Selection Process for Hard-Rock Mining. SME mining engineering Handbook (Vol. 1). SME.

[16]. Laubscher, D.H. (1990). A geomechanics classification system for the rating of rock mass in mine design. Journal of the Southern African Institute of Mining and Metallurgy, 90(10), 257-273.

[17]. Mawdesley, C., Trueman, R. and Whiten, W.J. (2001). Extending the Mathews stability graph for open–stope design. Mining Technology. 110 (1): 27-39.

[18]. Stewart, S.B.V., and Forsyth, W.W. (1995). The Mathew's method for open stope design. CIM bulletin. 88 (992): 45-53.

[19]. Trueman, R., Mikula, P., Mawdesley, C. A., and Harries, N. (2000). Experience in Australia with the application of the Mathew's method for open stope design. The CIM Bulletin. 93 (1036): 162-167.

[20]. Mawdesley, C.A. (2002). Predicting rock mass cavability in block caving mines.

[21]. Tollenaar, R.N. (2008). Characterization of discrete fracture networks and their influence on caveability and fragmentation (Doctoral dissertation, University of British Columbia).

[22]. Barla, G., Boshkov, S. and Pariseau, W. (1980), Numerical modeling of block caving at the Grace Mine. Geo-mechanics applications in underground hard-rock mining, Turin, Italy, pp. 241-256.

[23]. Rech, W. and Lorig, L. (1992). Predictive numerical stress analysis of panel caving at the Henderson Mine. Proc. of MASSMIN, 92, 55-62.

[24]. Singh, U.K., Stephansson, O.J. and Herdocia, A. (1993). Simulation of progressive failure in hanging-

wall and footwall for mining with sub-level caving. Trans Instn Min Metall, Sect A: Min Industry, 102, A188-A194.

[25]. Karzulovic, A., Cavieres, P. and Pardo, C. (1999). Caving subsidence at El Teniente mine. Proceedings of SIMIN, 99.

[26]. Lorig, L. (2000). The Role of Numerical Modelling in Assessing Caveability, Itasca Consulting Group, Inc., Report to the International Caving Study: ICG00-099-3-16.

[27]. Trueman, R., Pierce, M. and Wattimena, R. (2002). Quantifying stresses and support requirements in the undercut and production level drifts of block and panel caving mines. International Journal of Rock Mechanics and Mining Sciences. 39 (5): 617-632.

[28]. Yasitli, N.E. and Unver, B. (2005). 3D numerical modeling of longwall mining with top-coal caving. International Journal of Rock Mechanics and Mining Sciences. 42 (2): 219-235.

[29]. Pierce, M., Cundall, P., Mas Ivars, D., Darcel, C., Young, R.P., Reyes-Montes, J. and Pettitt, W. (2006). Mass Mining Technology Project: Six Monthly Technical Report, Caving Mechanics, Sub-Project No. 4.2: Research and Methodology Improvement, and Sub-Project 4.3, Case Study Application. ICG06-2292-1-Tasks 2-3-14, Itasca Consulting Group, Inc., Minneapolis.

[30]. Beck, D., Reusch, F. and Arndt, S. (2007). Estimating the Probaaility of Mining-Induced Seismic Events using Mine-Scale, Inelastic Numerical Models. In Deep Mining 2007: Proceedings of the Fourth International Seminar on Deep and High Stress Mining (pp. 31-41). Australian Centre for Geomechanics.

[31]. Singh, G.S.P. and Singh, U.K. (2010). Numerical modeling study of the effect of some critical parameters on caving behavior of strata and support performance in a long-wall working. Rock Mechanics and Rock Engineering, 43(4), 475-489.

[32]. Woo, K. S., Eberhardt, E., Rabus, B., Stead, D. and Vyazmensky, A. (2012). Integration of field characterisation, mine production and InSAR monitoring data to constrain and calibrate 3-D numerical modelling of block caving-induced subsidence. International Journal of Rock Mechanics and Mining Sciences, 53, 166-178.

[33]. Cumming-Potvin, D., Wesseloo, J., Pierce, M.E., Garza-Cruz, T., Bouzeran, L., Jacobsz, S.W. and Kearsley, E. (2018, October). Numerical simulations of a centrifuge model of caving. In Caving 2018: Proceedings of the Fourth International Symposium on Block and Sublevel Caving (pp. 191-206). Australian Centre for Geomechanics.

[34]. Öge, İ.F. (2018). Prediction of top coal cavability character of a deep coal mine by empirical and

numerical methods. Journal of Mining Science. 54 (5): 793-803.

[35]. Xia, Z., Tan, Z., Pei, Q. and Wang, J. (2019). Ground pressure damage evolution mechanism of extraction level excavations induced by poor undercutting in block caving method. Geotechnical and Geological Engineering. 37 (5): 4461-4472.

[36]. Xia, Z., Tan, Z. and Miao, Y. (2020). Damage evolution mechanism of extraction structure during mining gently dipped orebody by block caving method. Geotechnical and geological engineering, 38(4), 3891-3902.

[37]. Lorig, L.J., Board, M.P., Potyondy, D.O. and Coetzee, M. J. (1995). Numerical modelling of caving using continuum and micro-mechanical models. In Proc. of CAMI'95 Canadian Conference on Computer Applications in the Mining Industry, Montreal, Qebec, Kanada (pp. 416-424).

[38]. Gilbride, L.J., Free, K.S., and Kehrman, R. (2005). Modeling Block Cave Subsidence at the Molycorp, Inc., Questa Mine? A Case Study. In Alaska Rocks 2005, The 40th US Symposium on Rock Mechanics (USRMS). OnePetro.

[39]. Kalenchuk, K.S., McKinnon, S. and Diederichs, M.S. (2008). Block geometry and rockmass characterization for prediction of dilution potential into sub-level cave mine voids. International Journal of Rock Mechanics and Mining Sciences. 45 (6): 929-940.

[40]. Xie, Y.S. and Zhao, Y.S. (2009). Numerical simulation of the top coal caving process using the discrete element method. International Journal of Rock Mechanics and Mining Sciences. 46 (6): 983-991.

[41]. Sharrock, G., Vakili, A., Duplancic, P. and Hastings, N. (2011). Numerical analysis of subsidence for Perserverence Deeps Block Cave in Continuum and Distinct Element Numerical Modelling in Geomechanics. Sainsbury, Hart, Detournay and Nelson (eds.), Paper, 06-03.

[42]. Gao, F., Stead, D. and Coggan, J. (2014). Evaluation of coal longwall caving characteristics using an innovative UDEC Trigon approach. Computers and Geotechnics, 55, 448-460.

[43]. Rafiee, R., Ataei, M., KhalooKakaie, R., Jalali, S. E., Sereshki, F. and Noroozi, M. (2018). Numerical modeling of influence parameters in cavabililty of rock mass in block caving mines. International Journal of Rock Mechanics and Mining Sciences, 105, 22-27.

[44]. Song, Z. and Konietzky, H. (2019). A particle-based numerical investigation on longwall top coal caving mining. Arabian Journal of Geosciences. 12 (18): 1-18.

[45]. Wang, J., Wei, W., Zhang, J., Mishra, B. and Li, A. (2020). Numerical investigation on the caving mechanism with different standard deviations of top

coal block size in LTCC. International Journal of Mining Science and Technology. 30 (5): 583-591.

[46]. Vyazmensky, A., Elmo, D., Stead, D. and Rance, J.R. (2007, May). Combined finite-discrete element modelling of surface subsidence associated with block caving mining. In 1st Canada-US Rock Mechanics Symposium. OnePetro.

[47]. Vyazmensky, A., Elmo, D. and Stead, D. (2010). Role of rock mass fabric and faulting in the development of block caving induced surface subsidence. Rock mechanics and rock engineering. 43 (5): 533-556.

[48]. Rance, J.M., Van As, A., Owen, D.R.J., Feng, Y.T., and Pine, R. J. (2007). Computational modeling of multiple fragmentation in rock masses with application to block caving. In 1st Canada-US Rock Mechanics Symposium. OnePetro.

[49]. Mohammadi, S., Ataei, M., Kakaie, R., Mirzaghorbanali, A. and Aziz, N. (2021). A Probabilistic Model to Determine Main Caving Span by Evaluating Cavability of Immediate Roof Strata in Longwall Mining. Geotechnical and Geological Engineering. 39 (3): 2221-2237.

[50]. Ivars, D.M., Pierce, M.E., Darcel, C., Reyes-Montes, J., Potyondy, D.O., Young, R.P., and Cundall, P.A. (2011). The synthetic rock mass approach for jointed rock mass modelling. International Journal of Rock Mechanics and Mining Sciences. 48 (2): 219-244.

[51]. Karekal, S., Das, R., Mosse, L. and Cleary, P.W. (2011). Application of a mesh-free continuum method for simulation of rock caving processes. International Journal of Rock Mechanics and Mining Sciences. 48 (5): 703-711.

[52]. Park, D.W., and Kicker, D.C. (1985). Physical model study of a longwall mine. Mining Science and Technology. 3 (1): 51-61.

[53]. Kang, H., Li, J., Yang, J. and Gao, F. (2017). Investigation on the influence of abutment pressure on the stability of rock bolt reinforced roof strata through physical and numerical modeling. Rock Mechanics and Rock Engineering. 50 (2): 387-401.

[54]. McNearny, R.L., and Abel Jr, J.F. (1993). Large-scale two-dimensional block caving model tests. In International journal of rock mechanics and mining

sciences and geomechanics abstracts (Vol. 30, No. 2, pp. 93-109). Pergamon.

[55]. Carmichael. P. and Hebblewhite. B. (2012). An investigation into semi-intact rock mass representation for physical modelling block caving mechanics zone. Mining education Australian Research projects review.

[56]. Cumming-Potvin, D., Wesseloo, J., Jacobsz, S.W., and Kearsley, E. (2016). Results from physical models of block caving. In 7th International Conference and Exhibition on Mass Mining (MassMin 2016), 9-11 May 2016, Sydney, New South Wales, Australia (pp. 329-340). Australasian Institute of Mining and Metallurgy.

[57]. Jacobsz, S.W., Kearsley, E.P., Cumming-Potvin, D. and Wesseloo, J. (2018). Modelling cave mining in the geotechnical centrifuge. In Physical Modeling in Geotechnics, The 9th International Conference on Physical Modelling in Geotechnics (ICPMG 2018) (pp. 809-814).

[58]. Bai, Q., Tu, S. and Wang, F. (2019). Characterizing the top coal cavability with hard stone band (s): insights from laboratory physical modeling. Rock Mechanics and Rock Engineering. 52 (5): 1505-1521.

[59]. Heydarnoori, V., Khosravi, M.H. and Bahaaddini, M. (2020). Physical modelling of caving propagation process and damage profile ahead of the cave-back. Journal of Mining and Environment. 11 (4): 1047-1058.

[60]. Rafiee, R., Ataei, M., KhaloKakaie, R., Jalali, S.E. and Sereshki, F. (2016). A fuzzy rock engineering system to assess rock mass cavability in block caving mines. Neural Computing and Applications. 27 (7): 2083-2094.

[61]. Azadmehr, A., and Jalali, S.M.E. (2017). Assessment of rock mass caveability in block caving mining method, using Rock Engineering Systems (RES). Tunneling and Underground Space Engineering. 6 (1): 57-78.

[62]. Rafiee, R., Ataei, M., Khalokakaie, R., Jalali, S.M.E., and Sereshki, F. (2015). Determination and assessment of parameters influencing rock mass cavability in block caving mines using the probabilistic rock engineering system. Rock Mechanics and Rock Engineering. 48 (3): 1207-1220.

تعیین شعاع هیدرولیکی تخریب توده‌سنگ در روش تخریب بزرگ با استفاده از مدلسازی عددی و رگرسیون‌گیری چند متغیره

بهنام علی پنهانی، عباس مجدی* و حسن بخشنده امنیه

بخش مهندسی معدن، دانشگاه تهران، تهران، ایران

* نویسنده مسئول مکاتبات: amajdi@ut.ac.ir

چکیده:

تعیین شعاع هیدرولیکی زیربرش در روش تخریب بزرگ یکی از موضوعات کلیدی در این روش به شمار می‌رود. شعاع هیدرولیکی به‌طور مستقیم با حداقل دهانه تخریب در ارتباط است. در این تحقیق، قابلیت تخریب توده‌سنگ با استفاده از نرم‌افزارهای UDEC و 3DEC بررسی شده است. از آنجاکه عوامل موثر بر قابلیت تخریب بسیار متنوع و زیاد هستند، پس از مدلسازی دو بعدی در نرم‌افزار UDEC و بررسی روند تغییرات حداقل دهانه تخریب برحسب هر متغیر با ثابت نگه داشتن سایر متغیرها (بررسی تک عاملی)، از میان عومل مختلف، مهم‌ترین عوامل شامل عمق، شیب دسته درزه‌ها، تعداد دسته درزه‌ها، زاویه اصطکاک سطح درزه و فاصله‌داری درزه‌ها برای بررسی نهایی انتخاب شدند. در مرحله بعدی، رابطه حداقل دهانه تخریب برای پنج عامل اصلی و مقادیر معین شده در بررسی تک عاملی، با استفاده از نرم‌افزار SPSS و با انجام رگرسیون گیری چند متغیره تعیین شد. تابع توانی تغییرات حداقل دهانه تخریب براساس متغیرهای انتخابی با ضریب تعیین ۰/۷۶ انتخاب شد. در ادامه مدل سه بعدی ساده‌ای از زیربرش ساخته شد. بین نتایج مدلسازی دو بعدی و سه بعدی در شرایط مشابه رابطه خطی به‌دست آمد. در یک مدل با شرایط مشخص، شعاع هیدرولیکی حاصل از رابطه به دست آمده از روش عددی ۲۲/۵ متر است که به نتیجه حاصل از روش تجربی لابسچر در همان شرایط (۲۴ متر) نزدیک است.

کلمات کلیدی: قابلیت تخریب، حداقل دهانه تخریب، روش عددی، رگرسیون چند متغیره.